Hindawi Publishing Corporation
EURASIP Journal on Wireless Communications and Networking
Volume 2008, Article ID 549371, 14 pages
doi:10.1155/2008/549371

Research Article

Interference Robust Transmission for the Downlink of an OFDM-Based Mobile Communications System

Markus Konrad and Wolfgang Gerstacker

Institute of Mobile Communications, University of Erlangen-Nuremberg, Cauerstrasse 7, 91058 Erlangen, Germany

Correspondence should be addressed to Markus Konrad, konrad@lnt.de

Radio networks for future mobile communications systems, for example, 3GPP Long-Term Evolution (LTE), are likely to use an orthogonal frequency division multiplexing- (OFDM-) based air interface in the downlink with a frequency reuse factor of one to avoid frequency planning. Therefore, system capacity is limited by interference, which is particularly crucial for mobile terminals with a single receive antenna. Nevertheless, next generation mobile communications systems aim at increasing downlink throughput. In this paper, a single antenna interference cancellation (SAIC) algorithm is introduced for amplitude-shift keying (ASK) modulation schemes in combination with bit-interleaved coded OFDM. By using such a transmission strategy, high gains in comparison to a conventional OFDM transmission with quadrature amplitude modulation (QAM) can be achieved. The superior performance of the novel scheme is confirmed by an analytical bit-error probability (BEP) analysis of the SAIC receiver for a single interferer, Rayleigh fading, and uncoded transmission. For the practically more relevant multiple interferer case we present an adaptive least-mean-square (LMS) and an adaptive recursive least-squares (RLS) SAIC algorithm. We show that in particular the RLS approach enables a good tradeoff between performance and complexity and is robust even to multiple interferers.

1. INTRODUCTION

Next generation mobile communications air interfaces, such as 3GPP Long-Term Evolution (LTE) [1] or WiMax [2], will employ orthogonal frequency division multiplexing (OFDM) for transmission in the downlink. In order to avoid frequency planning, a frequency reuse factor of one is envisaged for 3GPP LTE. Hence, with conventional receivers without interference suppression capabilities, transmission is possible only with relatively low data rates due to the resulting capacity limitation which contradicts the desire for high downlink data rates.

For this reason, interference cancellation and suppression has been and is a vivid area of research, and various contributions for OFDM transmission have already been made. In [3], interference suppression for synchronous and asynchronous cochannel interferers is studied. At the receiver side, an adaptive antenna array is employed which performs minimum mean-squared error (MMSE) diversity combining in order to exploit receive diversity. The approach introduced in [4] aims at optimizing the receive signal-to-interference-plus-noise ratio (SINR). The authors show that SINR based maximum ratio combining yields significant gains with respect to pure SNR optimization. Receive antenna diversity based interference suppression is also proposed in [5], where the presented solution is suited for time-invariant and time-variant channels. This is due to a two-stage structure comprising spatial diversity and constraint-based beamforming. In [6, 7], transmit and receive antenna diversity have been exploited in MIMO OFDM systems. Cochannel interference is suppressed in order to increase the user data rates and the number of users who can access the system. In [6] the focus lies on spatial multiplexing whereas in [7] solutions for space-time-coded MIMO systems involving beamforming are developed.

OFDM transmission with real-valued data symbols has been studied in [8], where an equalizer for suppression of intercarrier interference resulting from the time-variance of the mobile radio channel has been introduced which exploits the fact that the transmitted symbols are one-dimensional.

However, cochannel interference and channel coding were not taken into account.

As indicated above, multiple receive antennas are advantageous for cancellation of cochannel interference. However, due to cost and size limitations it is still a challenge to include more than one transmit antenna into a mobile terminal. Therefore, single antenna interference cancellation (SAIC) algorithms have received significant attention in academia and industry in recent years, especially for transmission with single-carrier modulation (cf. [9–11]). The benefits of SAIC were analyzed in [12] for GSM radio networks, and it has been shown that GSM network capacity can be dramatically improved by SAIC.

In this paper, we propose an SAIC algorithm for OFDM transmission, extending the approach in [13–15], referred to as mono-interference cancellation (MIC) to the downlink of an OFDM based air interface. For this scheme, real-valued amplitude-shift keying (ASK) modulation is used and additional channel coding is considered. Independent complex filtering with subsequent projection for interference removal is applied to each OFDM subcarrier. We present a zero-forcing (ZF) approach, the analytical MMSE solution, and also adaptive approaches which are based on the least-mean-square (LMS) and the recursive least-squares (RLS) algorithm, respectively. It turns out that the RLS algorithm is particularly suited for practical implementation.

In principle, real-valued ASK modulation has the drawback of being less power efficient than a corresponding complex quadrature amplitude modulation (QAM) constellation as the constellation points cannot be packed as densely in the complex plane as for QAM. However, since only one real dimension is used for data transmission, additional degrees of freedom are available which can be exploited for interference suppression at the receiver. In [16] it was demonstrated that transmission with real-valued data symbols can lead to a higher spectral efficiency for DS-CDMA transmission than using a complex symbol alphabet. In [17] widely linear equalization and blind channel identification using a minimum energy output energy adaptation algorithm is proposed for OFDM transmission impaired by narrowband interference.

We show that the improved possibilities for interference suppression in case of real-valued symbols more than compensate for the loss in power efficiency and even significant gains are possible in an interference limited environment with respect to a conventional OFDM scheme employing coded QAM modulation with the same spectral efficiency. Performance of a QAM scheme in principle could be enhanced by successive interference cancellation (SIC) [18]. However, due to the presence of multiple interferers in practical applications, SIC alone could not achieve an acceptable performance and hence, it would have to be combined with successive decoding [18]. Unfortunately, because desired signal and interferers are usually not frame aligned and the code laws of the interferers are not known in general, successive decoding is not applicable here.

In principle, optimum soft-output multiuser detection (MUD) without considering the code laws is a further alternative. However, in [18], Verdú showed that the computational complexity of an optimum multiuser detector increases exponentially with the number of users. In addition, the complexity of such a detector increases with the size of the modulation alphabet, which becomes particularly crucial for 16QAM and 64QAM transmission. Thus, MUD seems to be prohibitively complex for mobile terminals, assuming spectrally efficient OFDM transmission.

For these reasons, we do not consider interference suppression for conventional QAM transmission as this can be accomplished only by MUD or SIC for a single receive antenna. Instead, we use a low-complexity suboptimum detector equipped with a ZF equalizer for each subcarrier. For equalizer design, perfect channel knowledge is assumed.

For both schemes convolutional coding (CC) and bit-wise interleaving over time and frequency are employed and comparisons are made for equal spectral efficiency. For the QAM scheme a lower code rate R_c is applied in comparison to the ASK scheme in order to obtain the same spectral efficiency. Since for QAM no interference cancellation is applied, a higher coding gain ensures reasonable, however, in most cases inferior performance in comparison to the ASK scheme, as will be demonstrated.

In order to support the simulation results for the adaptive SAIC algorithm for coded and bit-interleaved OFDM transmission, we provide an analysis of the raw bit-error probability (BEP) of both schemes before channel decoding. The results confirm that significant gains are possible for M-ary ASK transmission in comparison to M^2-ary QAM transmission.

The remainder of the paper is organized as follows. In Section 2, the system model is introduced. In Section 3, we present an SAIC scheme for OFDM. A ZF- and an MMSE-SAIC approach are introduced, respectively, and adaptive SAIC solutions are presented. Section 4 provides a theoretical analysis of subcarrier BEP of ZF-SAIC for uncoded transmission over a Rayleigh fading channel and a single interferer. Simulation results are presented in Section 5 for the multiple interferer case applying both analytical and adaptive MMSE SAIC approaches in an LTE-related scenario for M-ary ASK transmission. A comparison to conventional QAM transmission with ZF equalization is provided which again shows the superior performance of ASK combined with SAIC. Section 6 summarizes the paper and presents our conclusions.

2. SYSTEM MODEL

Since only a single receive antenna is available, the class of interference cancellation algorithms exploiting receive diversity is excluded here. In the considered scenario a mobile terminal is impaired by additive white Gaussian noise and J cochannel interferers representing surrounding base stations. The interferers are present on all subcarriers of the desired signal. The transmission is protected by CC with code rate R_c and block interleaving with interleaving depth I_B. Subsequent linear modulation for the OFDM subcarriers uses real-valued coefficients (e.g., M-ary ASK modulation; M: size of

modulation alphabet) for both desired and interferer signals which are assumed to employ the same modulation alphabet.

For OFDM transmission, a rectangular pulse shaping filter is applied and a guard interval (GI) of sufficient duration is used such that intersymbol interference (ISI) can be avoided. The GI contains a cyclic extension of the transmit sequence such that the convolution of the discrete-time channel impulse response and the transmit sequence becomes cyclic at the receiver side after elimination of the GI and can be represented by a multiplication in discrete-frequency domain [19]. Thus, subcarrier μ of the ith receive signal block represented in discrete-frequency domain is given by

$$R_i[\mu] = H_i[\mu]A_i[\mu] + \sum_{j=1}^{J} G_{j,i}[\mu]B_{j,i}[\mu] + N_i[\mu], \qquad (1)$$

where i is the OFDM symbol index and j is the interferer index, $1 \le j \le J$. The discrete-time channel impulse responses comprising the effects of transmit filtering, the mobile channel, and receive filtering for the desired signal and the interferer signals are assumed to be mutually independent and constant during the transmission of a data frame but changing randomly from frame to frame (block fading). The corresponding discrete-frequency responses are $H_i[\mu]$ and $G_{j,i}[\mu]$ for the desired signal and the interferers, respectively. $A_i[\mu]$ and $B_{j,i}[\mu]$ denote the i.i.d. real-valued data symbols of desired user and interferers, respectively, at symbol time i and subcarrier frequency μ. The receiver noise is modeled by a white Gaussian process with one-sided noise power density N_0 and is represented in frequency domain by $N_i[\mu]$. For (1) it has been assumed that the OFDM symbols of desired signal and interferers are time-aligned, that is, the network is synchronous, as, for example, in [20]. Furthermore, perfect frequency synchronization has been assumed.

3. INTERFERENCE SUPPRESSION FOR OFDM TRANSMISSION

In [13–15] an approach for SAIC was introduced for application in the GSM system where the interfering signal is eliminated by complex filtering and subsequent projection of the filtered signal onto an arbitrary nonzero complex number c for the case of a single interferer. In the presence of multiple interferers, the filter coefficients are optimized such that the variance of the difference between the signal after projection and the desired signal is minimized, that is, an MMSE criterion is applied, guaranteeing interference suppression at minimum noise enhancement. The algorithm has been derived for flat fading as well as frequency-selective fading channels. As in an OFDM system the channel can be considered as flat for each subcarrier, the variant of the algorithm for flat fading is directly applicable to each subcarrier, and the required filter order of the complex filter $P_i[\mu]$ for subcarrier μ is zero. We denote the real-valued output signal of projection by $Y_i[\mu]$. The error signal, consisting of noise and residual interference, is given by

$$E_i[\mu] = Y_i[\mu] - A_i[\mu] = \mathcal{P}_c\{P_i[\mu]R_i[\mu]\} - A_i[\mu], \qquad (2)$$

where $\mathcal{P}_c\{x\}$ denotes projection of x onto an arbitrary nonzero complex number c and is given by

$$\mathcal{P}_c\{x\} = \frac{\mathrm{Re}\{x \cdot c^*\}}{|c|^2} \qquad (3)$$

(cf. [13–15]), and we also introduce $c^\perp = \mathrm{Im}\{c\} - j\mathrm{Re}\{c\}$ and note that the inner product of c and $c^\perp$ when interpreted as two-dimensional vectors is 0 ($\mathrm{Re}\{\cdot\}$: real part of a complex number; $\mathrm{Im}\{\cdot\}$: imaginary part of a complex number).

3.1. ZF solution

Under the presence of only a single interferer, that is, $J = 1$, and assuming perfect channel knowledge we can apply a ZF solution for $P_i[\mu]$. The projection of the filtered received signal $R_i[\mu]$ can be expressed as [15]

$$\mathcal{P}_c\{P_i[\mu]R_i[\mu]\} = \frac{\mathrm{Re}\{P_i[\mu]H_i[\mu]c^*\}}{|c|^2}A_i[\mu]$$
$$+ \frac{\mathrm{Re}\{P_i[\mu]G_{1,i}[\mu]c^*\}}{|c|^2}B_{1,i}[\mu] \qquad (4)$$
$$+ \frac{\mathrm{Re}\{P_i[\mu]N_i[\mu]c^*\}}{|c|^2}.$$

Without loss of generality, $c = 1$ is assumed for the following. Choosing $P_i[\mu]$ as

$$P_i[\mu] = c^\perp \frac{G_{1,i}^*[\mu]}{|G_{1,i}[\mu]|} = -j \cdot \frac{G_{1,i}^*[\mu]}{|G_{1,i}[\mu]|}, \qquad (5)$$

and using $c^\perp c^* = -j$ results in

$$\mathcal{P}_c\{P_i[\mu]R_i[\mu]\} = \frac{\mathrm{Re}\{G_{1,i}^*[\mu]H_i[\mu]c^\perp c^*\}}{|G_{1,i}[\mu]|}A_i[\mu]$$
$$+ \frac{\mathrm{Re}\{G_{1,i}^*[\mu]G_{1,i}[\mu]c^\perp c^*\}}{|G_{1,i}[\mu]|}B_{1,i}[\mu]$$
$$+ \frac{\mathrm{Re}\{G_{1,i}^*[\mu]N_i[\mu]c^\perp c^*\}}{|G_{1,i}[\mu]|} \qquad (6)$$
$$= \mathrm{Im}\left\{\frac{G_{1,i}^*[\mu] \cdot H_i[\mu]}{|G_{1,i}[\mu]|}\right\}A_i[\mu]$$
$$+ \tilde{N}_i[\mu] = \tilde{H}_i[\mu]A_i[\mu] + \tilde{N}_i[\mu],$$

such that the interferer is perfectly cancelled. The effective channel coefficient for the desired signal after filtering and projection is given by

$$\tilde{H}_i[\mu] = \mathrm{Im}\left\{\frac{G_{1,i}^*[\mu]}{|G_{1,i}[\mu]|}H_i[\mu]\right\}. \qquad (7)$$

3.2. MMSE solution

For an MMSE approach, which is more suitable to suppress multiple interferers, the associated cost function is defined as

$$J(P_i[\mu]) \triangleq \mathcal{E}\{(\mathcal{P}_c\{P_i[\mu] \cdot R_i[\mu]\} - A_i[\mu])^2\}, \qquad (8)$$

where $\mathcal{E}\{\cdot\}$ is the expectation operator. Exploiting the fact that the cost function is convex we determine its minimum via the zeros of its derivative,

$$\frac{\partial}{\partial P^*[\mu]} J(P_i[\mu]) \overset{!}{=} 0. \qquad (9)$$

This results in

$$\frac{\partial J(P_i[\mu])}{\partial P_i^*[\mu]} = \Phi_{RR}[\mu]P_i[\mu] + \Phi_{R^*R}[\mu]P_i^*[\mu] - 2\,\varphi_{AR}[\mu] \overset{!}{=} 0, \qquad (10)$$

where $(\cdot)^*$ denotes complex conjugation. The expressions in (10) are defined by

$$\begin{aligned}
\Phi_{RR}[\mu] &= \mathcal{E}\{R_i[\mu]R_i^*[\mu]\} \\
&= \sigma_a^2 \cdot |H_i[\mu]|^2 + \sum_{j=1}^{J} \sigma_j^2 \cdot |G_{j,i}[\mu]|^2 + 2\sigma_n^2,
\end{aligned} \qquad (11)$$

$$\varphi_{AR}[\mu] = \mathcal{E}\{A_i[\mu]R_i^*[\mu]\} = \sigma_a^2 \cdot H_i^*[\mu], \qquad (12)$$

$$\begin{aligned}
\Phi_{R^*R}[\mu] &= \mathcal{E}\{(R_i^*[\mu])^2\} \\
&= \sigma_a^2 \cdot (H_i^*[\mu])^2 + \sum_{j=1}^{J} \sigma_j^2 \cdot (G_{j,i}^*[\mu])^2,
\end{aligned} \qquad (13)$$

where σ_a^2 and σ_j^2 ($1 \leq j \leq J$) denote the variances of desired signal and of interferer signal j, respectively, and σ_n^2 is the variance of the inphase component of the rotationally symmetric noise $N_i[\mu]$. The total interference power is $\sigma_I^2 = \sum_{j=1}^{J} \sigma_j^2$. By splitting (10) into real and imaginary part and after straightforward calculations we obtain the solution for the MMSE filter $P_i[\mu]$:

$$P_i[\mu] = 2\frac{\varphi_{AR}[\mu]\Phi_{RR}[\mu] - \varphi_{AR}^*[\mu]\Phi_{R^*R}[\mu]}{\Phi_{RR}^2[\mu] + |\Phi_{R^*R}[\mu]|^2}. \qquad (14)$$

Assuming that only a single interferer is present ($J = 1$) and $\sigma_n^2 \to 0$, we can simplify (14) and obtain

$$P_i[\mu] = -j \cdot \frac{G_{1,i}^*[\mu]}{\mathrm{Im}\{H_i[\mu]G_{1,i}^*[\mu]\}}, \qquad (15)$$

which is equivalent to the ZF solution presented in (5) apart from a scaling factor. The derivation of this result is provided in Appendix A. Hence, when noise is negligible the projection of the filtered received signal according to (6) results in

$$\begin{aligned}
\mathrm{Re}\bigg\{ &-j \cdot \frac{H_i[\mu]G_{1,i}^*[\mu]}{\mathrm{Im}\{H_i[\mu]G_{1,i}^*[\mu]\}} \bigg\} A_i[\mu] \\
&+ \mathrm{Re}\bigg\{ -j \cdot \frac{G_{1,i}[\mu]G_{1,i}^*[\mu]}{\mathrm{Im}\{H_i[\mu]G_{1,i}^*[\mu]\}} \bigg\} B_{1,i}[\mu] = A_i[\mu],
\end{aligned} \qquad (16)$$

where the interferer has been perfectly cancelled as for the ZF solution.

3.3. Adaptive approaches

In order to determine filter coefficients approximating the MMSE solution, several OFDM training symbols $A_i[\cdot]$ are required for LMS and RLS algorithm, respectively. However, only the desired user's training symbols have to be known, and the algorithm performs blind adaptation with respect to interference.

(1) LMS algorithm

After the training period, the filter coefficients $P_i[\mu]$ are fixed and used for complex filtering in the current transmission frame, assuming that the channel is time-invariant during each frame.

The filter update equation for the projection filter is given, for example, in [21]. Using the normalized version of the LMS algorithm to allow for an adaptive LMS step size parameter we obtain the following update rule for the projection filter coefficients $P_{i+1}[\mu]$:

$$P_{i+1}[\mu] = P_i[\mu] + \frac{\widetilde{\rho}}{M_x[\mu] + \epsilon} E_i[\mu] \cdot R_i^*[\mu], \qquad (17)$$

where $M_x[\mu]$ is the expected power of the filter input signal $R_i[\mu]$,

$$M_x[\mu] = \mathcal{E}\{|R_i[\mu]|^2\}. \qquad (18)$$

The parameter $\widetilde{\rho}$ has to be chosen as $0 < \widetilde{\rho} < 2$ to guarantee a convergence of the algorithm. The variable $\epsilon \ll 1$ is a small real number required for regularization.

The convergence of the LMS algorithm is quite slow and therefore the algorithm does not seem suitable for practical applications. In contrast, the recursive least-squares (RLS) algorithm exhibits better performance in terms of convergence speed. Furthermore, the misadjustment [21] of the LMS algorithm is dependent on the dominant-to-residual interference (DIR) ratio and is generally larger than that of the RLS algorithm.

(2) RLS algorithm

The major advantage of the RLS algorithm is an order of magnitude faster convergence than that of the LMS algorithm [21] such that also time-variant channels can be tracked. This renders the proposed cancellation scheme suitable for practical implementation. As for the LMS algorithm, each subcarrier is treated independently and, hence, complexity scales linearly with the number of subcarriers. The input vector of the algorithm per subcarrier μ is defined as

$$\mathbf{U}_i[\mu] = [\mathrm{Re}\{R_i[\mu]\} - \mathrm{Im}\{R_i[\mu]\}]^T, \qquad (19)$$

where $(\cdot)^T$ denotes transposition. The a priori error signal of the RLS algorithm is defined as the difference of desired signal and the output of projection of the filtered received signal,

$$\begin{aligned}
E_i[\mu] &= A_i[\mu] - \mathrm{Re}\{P_{i-1}[\mu]R_i[\mu]\} \\
&= A_i[\mu] - \mathbf{U}_i^T[\mu]\mathbf{P}_{i-1}[\mu].
\end{aligned} \qquad (20)$$

With definition of variables $\mathbf{U}_i[\mu]$ and $E_i[\mu]$, the RLS algorithm can be applied in the form given in [21].

4. ANALYSIS OF RAW BEP OF ZF-SAIC AND COMPARISON TO STANDARD QAM TRANSMISSION

In order to prove that significant gains can be obtained by the SAIC receiver in conjunction with real-valued modulation we first provide a closed-form analysis for uncoded transmission. The results also characterize performance of coded transmission before channel decoding (raw BEP). A single OFDM subcarrier with Rayleigh fading channel coefficient $H_i[\mu]$ and the presence of a single interferer using also real-valued modulation with channel coefficient $G_{1,i}[\mu]$ are assumed. The aim of this section is to provide a fundamental understanding of the performance of the SAIC scheme by deriving the BEP and comparing it to that of corresponding QAM schemes. The number of interferers is $J = 1$ and the interference power is given by σ_I^2.

The channel power of the desired user before filtering and projection is given by $\xi = |H_i[\mu]|^2$, where the probability density function (pdf) of ξ is $f_\xi(\xi) = e^{-\xi}$. The average receive signal power before filtering is given by $\sigma_a^2 \cdot \mathcal{E}\{|H_i[\mu]|^2\}$ and normalized to one, $\sigma_a^2 = \mathcal{E}\{|H_i[\mu]|^2\} = 1$, where σ_a^2 is the variance of the desired signal.

In the following, we omit the subcarrier index μ, interferer index j, and OFDM symbol index i for simplicity in $H_i[\mu]$ as well as in the interferer channel coefficient $G_{1,i}[\mu]$ and assume that both channel coefficients are known. Expanding the expression in (7) for the effective channel coefficient $\tilde{H}$ after ZF-SAIC projection results in

$$\tilde{H} = |H| \cdot \sin\left(\arg\{H\} - \arg\{G\}\right) = |H| \cdot \sin(\varphi), \quad (21)$$

where $\varphi = \arg\{H\} - \arg\{G\}$ is uniformly distributed with pdf

$$f_\varphi(\varphi) = \begin{cases} \dfrac{1}{2\pi}, & 0 \le \varphi < 2\pi, \\ 0, & \text{else} \end{cases} \quad (22)$$

($\arg\{\cdot\}$: argument operator). With $\xi = |H|^2$ and $\nu = \sin^2(\varphi)$ the received power after SAIC is a function of the random variables ξ and ν,

$$p(\nu, \xi) = \nu \cdot \xi, \quad (23)$$

which are mutually independent. The pdf of ν can be derived from the pdf of φ. With $\nu = \sin^2(\varphi)$ we obtain

$$\frac{d\nu}{d\varphi} = 2 \cdot \sin\varphi \cos\varphi. \quad (24)$$

By using

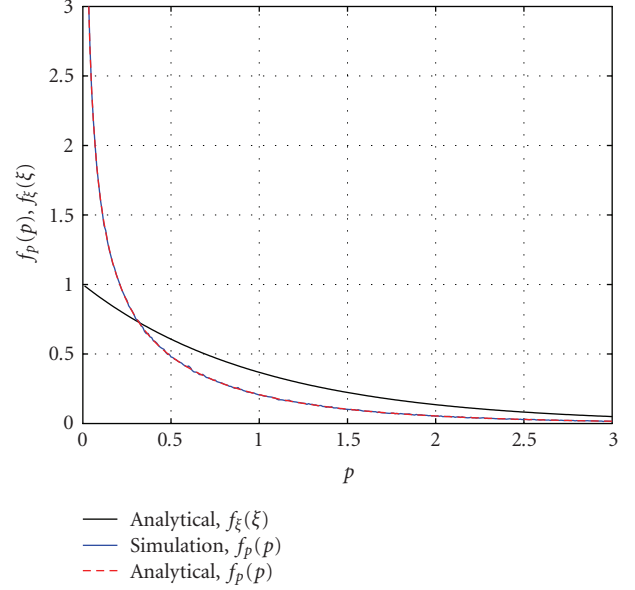$$\frac{1}{2\pi} d\varphi = \frac{1}{2\pi} \cdot \frac{1}{2 \cdot \sin\varphi \cos\varphi} d\nu, \quad (25)$$

FIGURE 1: Pdfs $f_\xi(\xi)$ and $f_p(p)$ of received power before and after ZF-SAIC, respectively.

— Analytical, $f_\xi(\xi)$
— Simulation, $f_p(p)$
- - - Analytical, $f_p(p)$

taking into account that $\varphi(\nu)$ is quadruple valued [22], using $\sqrt{\nu} = |\sin\varphi|$ and $|\cos\varphi| = \sqrt{1 - \sin^2(\varphi)}$, we obtain

$$f_\nu(\nu) = \begin{cases} \dfrac{1}{\pi} \cdot \dfrac{1}{\sqrt{\nu(1 - \nu)}}, & \text{for } 0 < \nu < 1, \\ 0, & \text{else.} \end{cases} \quad (26)$$

The joint pdf $f_{\nu,\xi}(\nu, \xi) = f_\nu(\nu) \cdot f_\xi(\xi)$ is needed to calculate the pdf of the product $p(\nu, \xi) = \nu \cdot \xi$ resulting in

$$\begin{aligned} f_p(p) &= \int_0^1 f_{\nu,\xi}\left(\nu, \frac{p}{\nu}\right) \left|\frac{1}{\nu}\right| d\nu \\ &= \int_0^1 \frac{1}{\sqrt{\nu(1-\nu)}} \cdot \frac{e^{-p/\nu}}{\pi\nu} d\nu = \frac{1}{\sqrt{\pi}} \frac{e^{-p}}{\sqrt{p}}. \end{aligned} \quad (27)$$

According to Figure 1, the receive power after SAIC is more likely to attain small values than before SAIC, as can be easily seen by comparing with the pdf $f_\xi(\xi)$ representing the receive power before SAIC.

4.1. Average SINR gain for 2ASK transmission

Assuming perfect channel knowledge, the SAIC scheme removes the interferer perfectly, such that the average receive SINR after SAIC is given by

$$\text{SINR} = \frac{\sigma_a^2 \cdot E\{p\}}{\sigma_n^2}. \quad (28)$$

The average SINR before interference cancellation for ASK transmission is

$$\text{SINR}_0 = \frac{\sigma_a^2}{\sigma_n^2 + \sigma_I^2}. \quad (29)$$
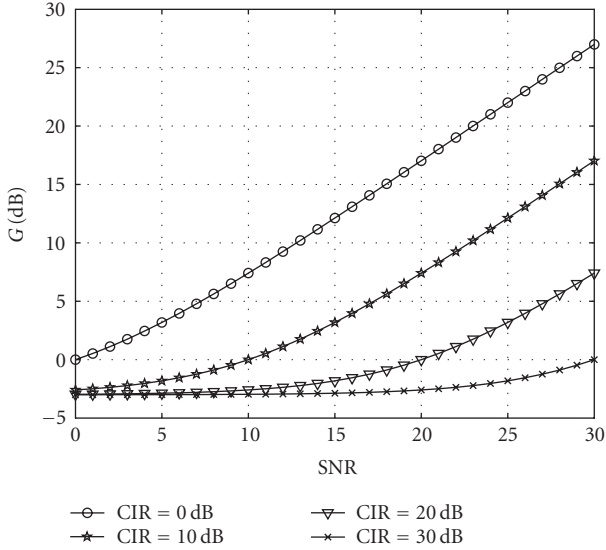
FIGURE 2: SINR gain of ZF-SAIC for ASK transmission versus SNR for different CIRs. A single interferer has been assumed.

The average receive power after SAIC can be calculated to

$$E\{p\} = \int_0^\infty p \cdot f_p(p)\, dp = \frac{1}{2}. \tag{30}$$

Hence, the SAIC scheme causes a 3 dB loss in receive power on average, but completely cancels the interference. In order to benefit from SAIC for ASK transmission the following condition has to be met:

$$\text{SINR} \geq \text{SINR}_0, \tag{31}$$

or

$$\frac{\sigma_a^2}{2\sigma_n^2} \geq \frac{\sigma_a^2}{\sigma_n^2 + \sigma_I^2}. \tag{32}$$

Hence, the proposed ZF-SAIC scheme is beneficial as long as

$$\sigma_I^2 \geq \sigma_n^2. \tag{33}$$

This is always fulfilled in the interference limited case, which we consider here. The gain in average SINR of the SAIC scheme compared to a standard ASK receiver can be expressed as

$$G = 10 \cdot \log_{10}\left(\frac{\sigma_I^2 + \sigma_n^2}{2\sigma_n^2}\right) \text{ [dB]} \tag{34}$$

and is depicted in Figure 2, where the SNR is defined as σ_a^2/σ_n^2. Figure 2 demonstrates that large SINR gains are possible by using SAIC in comparison to conventional zero-forcing reception, particularly for high SNRs.

4.2. Closed-form BEP calculation for ZF-SAIC using M-ary ASK for transmission over Rayleigh fading channels

In the following, we derive closed form expressions for BEP after SAIC for M-ary ASK transmission. In particular, since

2ASK, 4ASK, and 8ASK are considered in the simulations of Section 5 we provide the corresponding analytical formulas here.

In the following, the average subcarrier $\overline{E}_b/N_0$ is abbreviated by x, and the instantaneous subcarrier E_b/N_0 is abbreviated by y. Using (27), considering that $y = p \cdot x$, and applying a variable transform results in the pdf of y which is given by

$$f_y(y) = \frac{1}{\sqrt{\pi \cdot x}} \cdot \frac{e^{-(y/x)}}{\sqrt{y}}. \tag{35}$$

For the following BEP calculations the definition

$$G(M) = \frac{6\log_2 M}{2(M^2 - 1)} \tag{36}$$

is needed, with $G(2) = 1$, $G(4) = 2/5$, and $G(8) = 1/7$. The BEP for 2ASK for fixed instantaneous E_b/N_0 is given by [23]

$$P_b^{2\text{ASK}}(y) = \frac{1}{2}\text{erfc}\left(\sqrt{G(2)y}\right) = \frac{1}{2}\text{erfc}(\sqrt{y}). \tag{37}$$

For 4ASK the following BEP is obtained [24]:

$$P_b^{4\text{ASK}}(y) = \frac{2}{M\log_2 M} \cdot \left(\frac{3}{2}\text{erfc}\left(\sqrt{G(4)y}\right) + \text{erfc}\left(3 \cdot \sqrt{G(4)y}\right)\right.$$
$$\left. - \frac{1}{2}\text{erfc}\left(5 \cdot \sqrt{G(4)y}\right)\right)$$
$$= \frac{3}{8}\text{erfc}\left(\sqrt{\frac{2}{5}y}\right) + \frac{1}{4}\text{erfc}\left(\sqrt{\frac{18}{5}y}\right) - \frac{1}{8}\text{erfc}\left(\sqrt{10y}\right). \tag{38}$$

Finally, BEP for 8ASK reads [24]

$$P_b^{8\text{ASK}}(y) = \frac{7}{24}\text{erfc}\left(\sqrt{\frac{1}{7}y}\right)$$
$$+ \frac{1}{4}\text{erfc}\left(\sqrt{\frac{9}{7}y}\right) - \frac{1}{24}\text{erfc}\left(\sqrt{\frac{25}{7}y}\right) \tag{39}$$
$$+ \frac{1}{24}\text{erfc}\left(\sqrt{\frac{81}{7}y}\right) - \frac{1}{24}\text{erfc}\left(\sqrt{\frac{169}{7}y}\right).$$

The average raw BEP of the ZF-SAIC algorithm can be written as

$$\text{BEP} = \int_0^\infty P_b(y) f_y(y)\, dy. \tag{40}$$

Using Craig's formula [25],

$$\text{erfc}(\sqrt{x}) = \frac{2}{\pi}\int_0^{\pi/2}\exp\left(-\frac{x}{\sin^2(\theta)}\right)d\theta, \tag{41}$$

the BEP for M-ary ASK can be written as the sum of integrals over the same type of function. We need the identity

$$\int_0^\infty \text{erfc}\left(\sqrt{\alpha G(M)y}\right) f_y(y)\, dy$$
$$= \frac{1}{\sqrt{\pi x}}\frac{2}{\pi}\int_0^\infty\int_0^{\pi/2}\exp\left(-\frac{\alpha G(M)y}{\sin^2\theta}\right)$$
$$\times \exp\left(-\frac{y}{x}\right)y^{-(1/2)}\, d\theta\, dy \tag{42}$$
$$= \frac{1}{2}\left(1 - \frac{2}{\pi}\arctan\left(\frac{\alpha G(M)x - 1}{2\sqrt{\alpha G(M)x}}\right)\right),$$

where $\alpha \in \mathbb{R}^+$. The proof is given in Appendix B. Using (42), it is straightforward to show that the BEP of 2ASK after SAIC can be written as

$$\overline{P}_b^{2ASK}(x) = \frac{1}{4} - \frac{1}{2\pi} \arctan\left(\frac{x-1}{2\sqrt{x}}\right). \qquad (43)$$

The closed-form solution for the BEP of 4ASK is

$$\begin{aligned}
\overline{P}_b^{4ASK}(x) = {} & \frac{3}{16}\left(1 - \frac{2}{\pi}\arctan\left(\frac{(2/5)x - 1}{2\sqrt{(2/5)x}}\right)\right) \\
& + \frac{1}{8}\left(1 - \frac{2}{\pi}\arctan\left(\frac{(18/5)x - 1}{2\sqrt{(18/5)x}}\right)\right) \\
& - \frac{1}{16}\left(1 - \frac{2}{\pi}\arctan\left(\frac{10x - 1}{2\sqrt{10x}}\right)\right),
\end{aligned} \qquad (44)$$

where (38) and again (42) have been used, and for 8ASK we obtain

$$\begin{aligned}
\overline{P}_b^{8ASK}(x) = {} & \frac{7}{48}\left(1 - \frac{2}{\pi}\arctan\left(\frac{(1/7)x - 1}{2\sqrt{(1/7)x}}\right)\right) \\
& + \frac{1}{8}\left(1 - \frac{2}{\pi}\arctan\left(\frac{(9/7)x - 1}{2\sqrt{(9/7)x}}\right)\right) \\
& - \frac{1}{48}\left(1 - \frac{2}{\pi}\arctan\left(\frac{(25/7)x - 1}{2\sqrt{(25/7)x}}\right)\right) \\
& + \frac{1}{48}\left(1 - \frac{2}{\pi}\arctan\left(\frac{(81/7)x - 1}{2\sqrt{(81/7)x}}\right)\right) \\
& - \frac{1}{48}\left(1 - \frac{2}{\pi}\arctan\left(\frac{(169/7)x - 1}{2\sqrt{(169/7)x}}\right)\right)
\end{aligned} \qquad (45)$$

with (39) and (42). BEP after SAIC per subcarrier is depicted in Figure 3 versus the subcarrier $\overline{E}_b/N_0$.

In the following, we develop a low SNR approximation of BEP for 2ASK. With the trigonometric equivalence of [26]

$$\arctan\gamma = \arcsin\left(\frac{\gamma}{\sqrt{1+\gamma^2}}\right), \qquad (46)$$

we can rewrite

$$\begin{aligned}
\arctan\left(\frac{x-1}{2\sqrt{x}}\right) &= \arcsin\left(\frac{(x-1)/2\sqrt{x}}{\sqrt{1 + \left((x-1)/2\sqrt{x}\right)^2}}\right) \\
&= \arcsin\left(\frac{x-1}{x+1}\right).
\end{aligned} \qquad (47)$$

Thus, the alternative expression

$$\overline{P}_b^{2ASK}\left(\frac{\overline{E}_b}{N_0}\right) = \frac{1}{4} - \frac{1}{2\pi}\arcsin\left(\frac{\overline{E}_b/N_0 - 1}{\overline{E}_b/N_0 + 1}\right) \qquad (48)$$

follows from (43) and (47). For $\overline{E}_b/N_0 \approx 1$ we can approximate the BEP by using

$$\arcsin(y) \approx y \quad \text{for } |y| \ll 1, \qquad (49)$$

resulting in

$$\overline{P}_b^{2ASK}\left(\frac{\overline{E}_b}{N_0}\right) \approx \frac{1}{4} - \frac{1}{2\pi}\cdot\frac{\overline{E}_b/N_0 - 1}{\overline{E}_b/N_0 + 1}, \qquad (50)$$
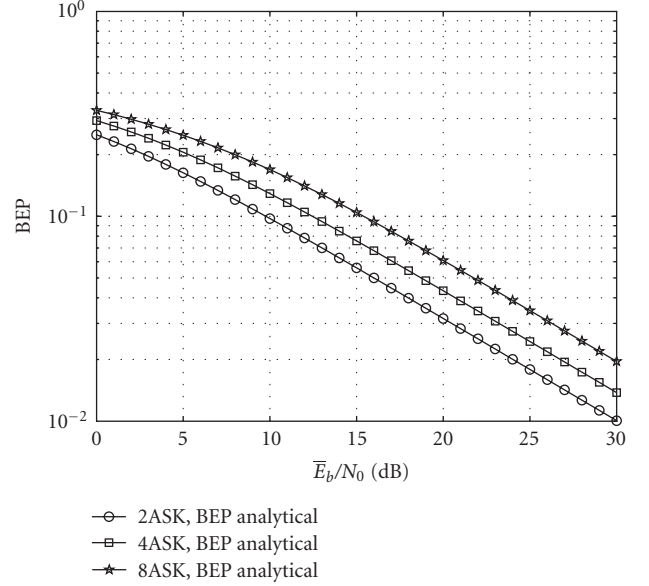

FIGURE 3: BEP after ZF-SAIC versus $\overline{E}_b/N_0$ for 2ASK, 4ASK, and 8ASK. A single interferer has been assumed.

or

$$\overline{P}_b^{2ASK}\left(\frac{\overline{E}_b}{N_0}\right) \approx \frac{1}{4} - \frac{1}{2\pi}\cdot\left(\frac{\overline{E}_b/N_0 - 1}{2\sqrt{\overline{E}_b/N_0}}\right), \qquad (51)$$

exploiting the equivalence in (47). The exact BEP, the simulated raw BER, and both low SNR BEP approximations are shown in Figure 4 for a carrier-to-interference ratio (CIR) of 10 dB, where CIR $= \sigma_a^2/\sigma_I^2$. Both approximations are in good agreement for $\overline{E}_b/N_0$ between -5 dB and 5 dB. Analytical and simulation results for BEP of 2ASK after SAIC match perfectly.

In the following, we determine the diversity order for M-ary ASK, that is, the slope of the BEP curve for $\overline{E}_b/N_0 \to \infty$ in a double-logarithmic representation. For M-ary ASK the average BEP can be expressed as

$$\overline{P}_b^{MASK}\left(\frac{\overline{E}_b}{N_0}\right) = \sum_i b_i \cdot t_i\left(\frac{\overline{E}_b}{N_0}\right), \qquad (52)$$

where

$$t_i\left(\frac{\overline{E}_b}{N_0}\right) = 1 - \frac{2}{\pi}\cdot\arctan\left(\frac{c_i(\overline{E}_b/N_0) - 1}{2\sqrt{c_i(\overline{E}_b/N_0)}}\right). \qquad (53)$$

For 2ASK, 4ASK, and 8ASK, respectively, the values of b_i and c_i can be extracted from the analytical formulas for BEP given in (43), (44), and (45).

For determining the diversity order we first consider $t_i(\overline{E}_b/N_0)$ for $(\overline{E}_b/N_0) \to \infty$. After substituting $\overline{E}_b/N_0$ by e^λ we obtain

$$\begin{aligned}
t_i(\lambda) &= 1 - \frac{2}{\pi}\arctan\left(\frac{c_i e^\lambda - 1}{2\sqrt{c_i e^\lambda}}\right) \\
&= 1 - \frac{2}{\pi}\arctan\left(\sinh\left(\frac{\ln c_i + \lambda}{2}\right)\right).
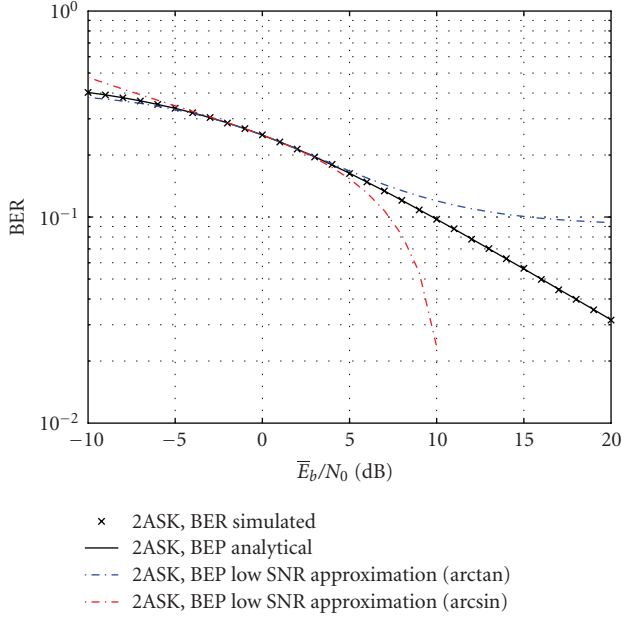\end{aligned} \qquad (54)$$

FIGURE 4: Analytical BEP, simulated BER, and low SNR approximations versus subcarrier $\overline{E}_b/N_0$ for ZF-SAIC. A single interferer has been assumed.

Subsequently, we have to calculate the limit of the derivative of the natural logarithm of $t_i(\lambda)$ with respect to λ for $\lambda \to \infty$. With

$$\ln\left(t_i(\lambda)\right) = \ln\left(1 - \frac{2}{\pi}\arctan\left(\sinh\left(\frac{\ln c_i + \lambda}{2}\right)\right)\right), \quad (55)$$

we obtain

$$\frac{d}{d\lambda}\ln\left(t_i(\lambda)\right) = -\frac{1}{\pi}\cdot\frac{\overbrace{\left(\cosh\left((\ln c_i + \lambda)/2\right)\right)^{-1}}^{\tilde{a}(\lambda)}}{\underbrace{1 - \frac{2}{\pi}\arctan\left(\sinh\left((\ln c_i + \lambda)/2\right)\right)}_{\tilde{b}(\lambda)}}. \quad (56)$$

Because $\lim_{\lambda \to \infty} \tilde{a}(\lambda) = 0$ and $\lim_{\lambda \to \infty} \tilde{b}(\lambda) = 0$ we have to apply L'Hospitale's rule in order to find the derivative. With

$$\tilde{a}'(\lambda) = -\frac{1}{2}\cdot\frac{\tanh\left((\ln c_i + \lambda)/2\right)}{\cosh\left((\ln c_i + \lambda)/2\right)},$$
$$\tilde{b}'(\lambda)| = -\frac{1}{\pi}\cdot\frac{1}{\cosh\left((\ln c_i + \lambda)/2\right)}, \quad (57)$$

the diversity order of $t_i(\overline{E}_b/N_0)$ is

$$-\lim_{\lambda \to \infty}\frac{d}{d\lambda}\ln\left(t_i(\lambda)\right) = \frac{1}{2} \quad \forall i, \quad (58)$$

which is independent of the constant c_i. We can express the limit of $t_i(\lambda)$ for $\lambda \to \infty$ as

$$\lim_{\lambda \to \infty} t_i(\lambda) = \lim_{\lambda \to \infty}\exp\left(\int\frac{d}{d\lambda}\ln\left(t_i(\lambda)\right) d\lambda\right)$$
$$= \lim_{\lambda \to \infty}\exp\left(-\frac{1}{2}\lambda + \tilde{c}_i\right) = e^{\tilde{c}_i}\cdot e^{-(1/2)\lambda}, \quad (59)$$

where $\tilde{c}_i$ is an integration constant. By using (52) and (59) we obtain the limit of the average BEP for $\lambda \to \infty$ as

$$\lim_{\lambda \to \infty}\overline{P}_b^{MASK}(\lambda) = \sum_i b_i\cdot\lim_{\lambda \to \infty} t_i(\lambda) = \sum_i b_i\cdot e^{\tilde{c}_i}\cdot e^{-(1/2)\lambda}$$
$$= C\cdot e^{-(1/2)\lambda}, \quad (60)$$

where

$$C = \sum_i b_i\cdot e^{\tilde{c}_i}, \quad C \in \mathbb{R}^+. \quad (61)$$

The diversity order for M-ary ASK is then given by

$$-\lim_{\lambda \to \infty}\frac{d}{d\lambda}\ln\left(\overline{P}_b^{MASK}(\lambda)\right) = -\lim_{\lambda \to \infty}\frac{d}{d\lambda}\left(\ln\left(C\cdot e^{-(1/2)\lambda}\right)\right) = \frac{1}{2} \quad (62)$$

for all ASK constellations considered in this paper.

4.3. M^2-ary QAM transmission over a Rayleigh fading channel with a single interferer

In the following, we assume that the interference can be modeled by a Gaussian random process with average variance σ_I^2. The average CIR is defined by the ratio of the power of the useful signal and that of the interferer signal, and both powers are exponentially distributed with mean values $\sigma_a^2 = 1$ and $\sigma_I^2 = 1/\text{CIR}$, respectively. The effective subcarrier E_b/N_0 for a given instantaneous CIR value, denoted by CIR_{inst}, is

$$\left(\frac{E_b}{N_0}\right)_{\text{eff}} = \frac{1}{1/(E_b/N_0) + (\log_2 M/\text{CIR}_{\text{inst}})}. \quad (63)$$

Closed-form expressions for the BEP in dependence on the subcarrier $\overline{E}_b/N_0$ for M^2-ary QAM (4QAM, 16QAM, and 64QAM) transmission over a Rayleigh fading channel are provided in Appendix C. Using these, we can determine the average BEP of QAM numerically for a given average CIR by inserting $(E_b/N_0)_{\text{eff}}$ in the respective formulas and averaging over CIR_{inst}. In Figures 5–7, the BEP performance versus $\overline{E}_b/N_0$ of M^2-ary QAM and M-ary ASK transmission is compared for $M = 2, 4$, and 8, respectively. M-ary ASK transmission with SAIC performs worse than M^2-ary QAM transmission for infinite CIR due to the reduced diversity degree of 1/2. However, for finite CIRs ASK transmission in combination with SAIC outperforms QAM transmission as long as the subcarrier $\overline{E}_b/N_0$ is above a certain threshold depending on CIR. Furthermore, the ASK BEP curves do not exhibit bit-error floors, in contrast to the QAM curves. For example, for a CIR of 10 dB, the proposed ASK scheme using SAIC outperforms the corresponding QAM transmission if $\overline{E}_b/N_0$ exceeds values of 25, 20, and 15 dB, respectively, for $M = 2, 4$, and 8 (cf. Figures 5–7). This analysis clearly shows that large gains can be obtained in an interference limited scenario by using the proposed scheme.

5. SIMULATION RESULTS FOR ADAPTIVE SAIC AND MULTIPLE INTERFERERS

The key parameters for the numerical results shown in this section are summarized in Table 1. A carrier frequency of
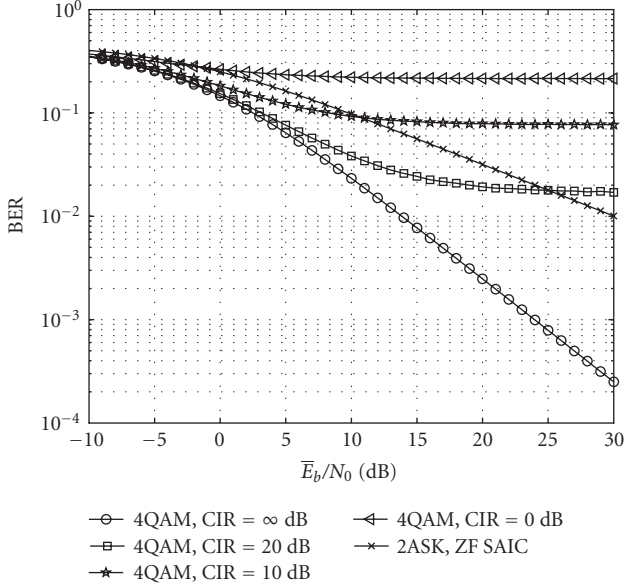
FIGURE 5: BEP for 2ASK and 4QAM transmission versus subcarrier $\overline{E}_b/N_0$ for different CIRs. A single interferer has been assumed.
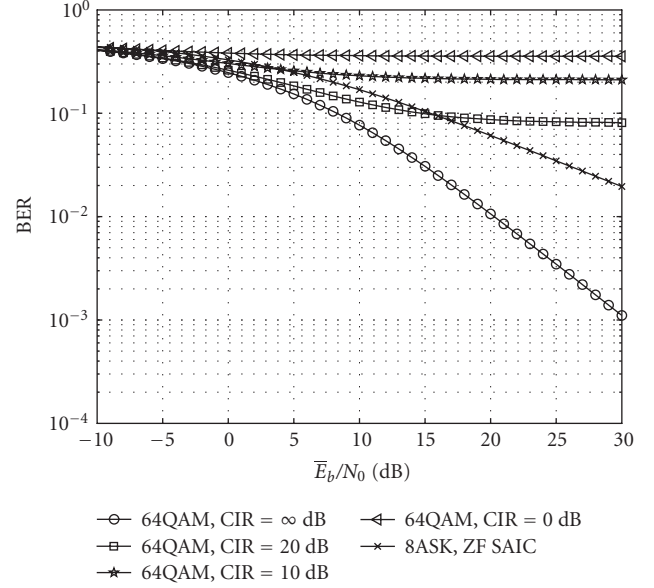

FIGURE 7: BEP for 8ASK and 64QAM transmission versus subcarrier $\overline{E}_b/N_0$ for different CIRs. A single interferer has been assumed.
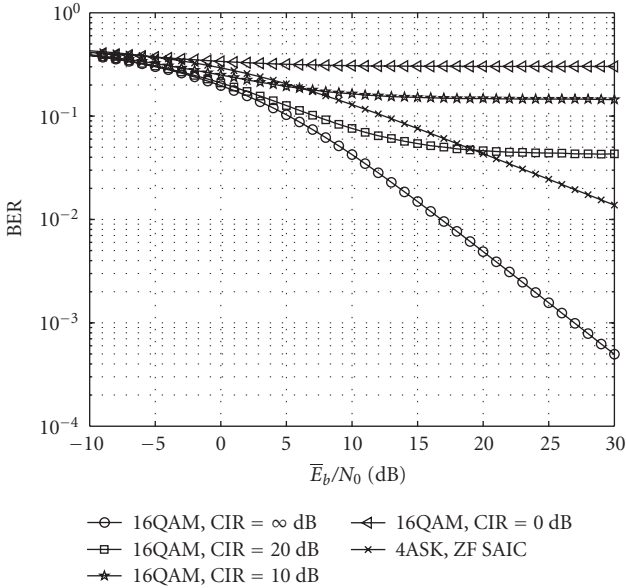

FIGURE 6: BEP for 4ASK and 16QAM transmission versus subcarrier $\overline{E}_b/N_0$ for different CIRs. A single interferer has been assumed.

TABLE 1: Simulation parameters.

Parameter	Value
Number of subcarriers	512
System bandwidth B	7.68 MHz
Code rates R_c	2/3, 1/2, 1/3, 1/4
Interleaving depth I_B	32 bits
Channel model	Typical urban [27]
Maximum channel excess delay	$\tau_{\max} = 7\,\mu s$
Number of interferers J	3
OFDM sample spacing	$T_s = 130.2$ ns
OFDM symbol duration	$T = 512 \cdot T_s = 66.67\,\mu s$
Length of guard interval T_G	$0.25 \cdot T$
Number of training symbols for the LMS algorithm	210
Normalized LMS step size parameter $\widetilde{\rho}$	0.2
Number of training symbols for the RLS algorithm	21
RLS forgetting factor λ [21]	0.99
Number of simulated channels	10^4

2 GHz is assumed, and the number of used OFDM subcarriers was set to 512. All subcarriers are impaired by cochannel interference and additive white Gaussian noise. In the following, $\overline{E}_b$ denotes the average receive energy per bit of the desired signal. The carrier-to-interference ratio is given by CIR $= C/I_t$, where C and I_t are the average receive power of the desired signal and of the total interference, respectively. In order to model the interference structure of a cellular network, $J = 3$ cochannel interferers are considered. One of the interferers dominates and has power I_d, whereas the other, residual interferers have equal average powers I_2 and

I_3. The total power of the residual interference is $I_r = I_2 + I_3$, and $I_t = I_d + I_r$. The dominant-to-residual-interference ratio (DIR) is defined as I_d/I_r.

The considered discrete-time channel impulse responses of desired signal and interferers have mutually uncorrelated Rayleigh fading taps with average tap powers according to an exponential power delay profile which is determined from the continuous typical urban power delay profile given in [27], $P(\tau) = e^{-\tau/\tau_0}$ for $0 \leq \tau \leq \tau_{\max} = 7\,\mu s$ and $P(\tau) = 0$ else, where $\tau_0 = 1\,\mu s$, by sampling with a sample spacing of $T_s = 130.2$ ns. A block fading model is adopted with random
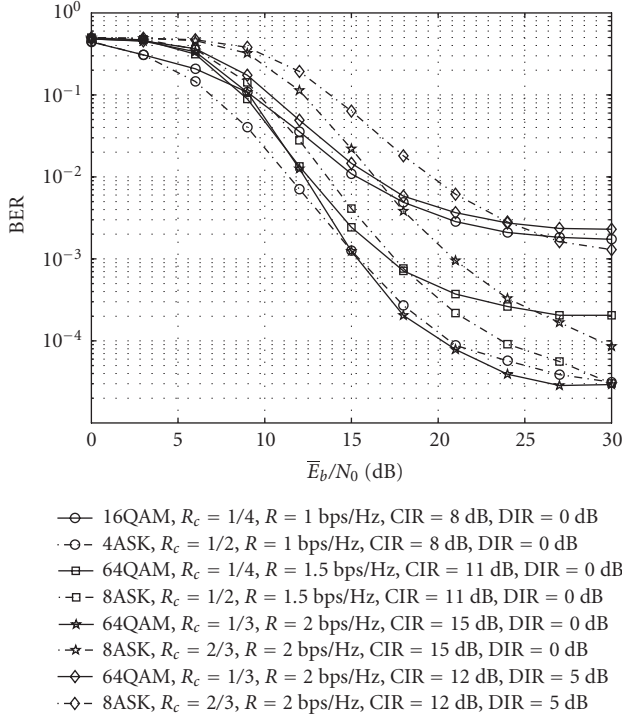
FIGURE 8: BER after channel decoding versus $\overline{E}_b/N_0$ for different transmission schemes and interference conditions.

- —○— 16QAM, $R_c = 1/4$, $R = 1$ bps/Hz, CIR = 8 dB, DIR = 0 dB
- ··○·· 4ASK, $R_c = 1/2$, $R = 1$ bps/Hz, CIR = 8 dB, DIR = 0 dB
- —□— 64QAM, $R_c = 1/4$, $R = 1.5$ bps/Hz, CIR = 11 dB, DIR = 0 dB
- ··□·· 8ASK, $R_c = 1/2$, $R = 1.5$ bps/Hz, CIR = 11 dB, DIR = 0 dB
- —★— 64QAM, $R_c = 1/3$, $R = 2$ bps/Hz, CIR = 15 dB, DIR = 0 dB
- ··★·· 8ASK, $R_c = 2/3$, $R = 2$ bps/Hz, CIR = 15 dB, DIR = 0 dB
- —◇— 64QAM, $R_c = 1/3$, $R = 2$ bps/Hz, CIR = 12 dB, DIR = 5 dB
- ··◇·· 8ASK, $R_c = 2/3$, $R = 2$ bps/Hz, CIR = 12 dB, DIR = 5 dB

FIGURE 9: BER after channel decoding versus CIR for varying DIR. 4ASK with $R_c = 0.5$ and 16QAM with $R_c = 0.25$, $R = 1$ bit/s/Hz. "an" stands for the analytical MMSE solution.

- —○— DIR = −5 dB, an
- —□— DIR = 0 dB, an
- —★— DIR = 5 dB, an
- —◇— DIR = 10 dB, an
- —△— DIR = 15 dB, an
- —◁— DIR = 20 dB, an
- ··○·· DIR = −5 dB, RLS
- ··□·· DIR = 0 dB, RLS
- ··★·· DIR = 5 dB, RLS
- ··◇·· DIR = 10 dB, RLS
- ··△·· DIR = 15 dB, RLS
- ··◁·· DIR = 20 dB, RLS
- –□– DIR = 0 dB, LMS
- –◇– DIR = 10 dB, LMS
- ×× QAM DIR = 0 dB

changes from frame to frame. Each frame consists of training blocks and data blocks. Each block comprises 7 OFDM symbols, and channel coding and interleaving are performed on each block.

The choice of simulation parameters used in this paper was to a large extent inspired by the 3GPP LTE standard [1]. The sampling rate of $1/T_s = 7.68$ MHz, the number of 512 subcarriers, the OFDM subcarrier bandwidth of 15 kHz, and the number of 7 OFDM symbols per block, respectively, conform with the downlink FDD specifications of the LTE standard. Furthermore, we confine the QAM constellation size to a maximum of $M^2 = 64$ as in [1] and the corresponding ASK constellation size to $M = 8$. However, instead of leaving a large part of the spectrum unused as proposed in [1], we use 512 modulated subcarriers per OFDM symbol, which results in a total system bandwidth of $B = 512 \cdot 15$ kHz $= 7.68$ MHz. The impulse response length of the typical urban channel $\tau_{max} = 7\,\mu$s exceeds the duration of the short guard interval as standardized in LTE for unicast transmission. For that reason we choose the long guard interval which has a length of 25% of the OFDM symbol duration in order to exclude intersymbol interference. Furthermore, we prefer convolutional coding to turbo coding to maintain a low receiver complexity. We use entire OFDM symbols as training symbols for the algorithms proposed in this paper as opposed to reference symbols as indicated in the LTE standard.

The performance results for the proposed scheme with ASK transmission and SAIC are compared with results for QAM transmission with ZF equalization. In this case, the receiver has perfect channel knowledge. For both schemes, in-
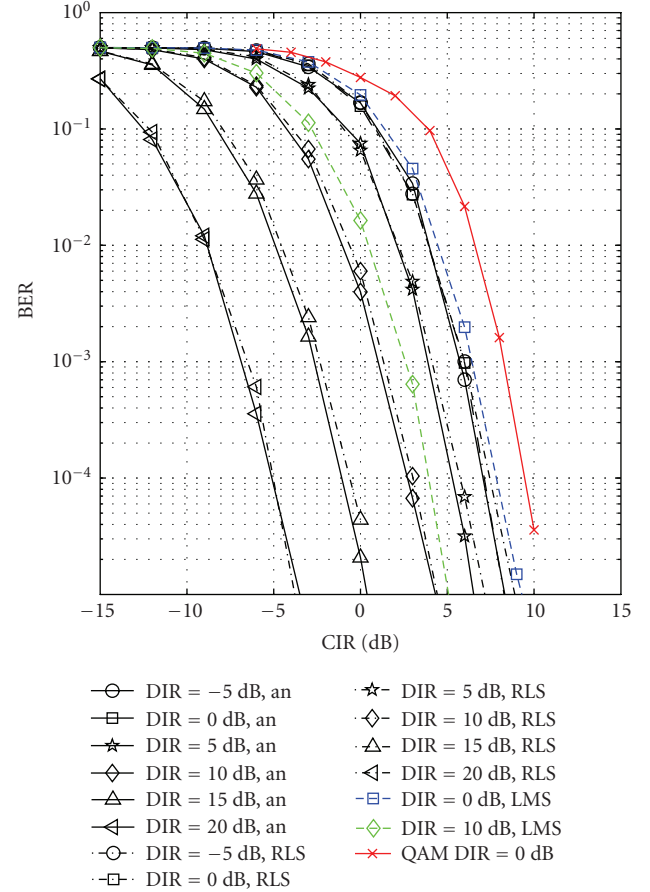
terleaving with interleaving depth I_B and CC with constraint length 9 is applied. Furthermore, in order to provide a fair comparison, QAM transmission is stronger protected by CC than ASK in order to obtain the same spectral efficiency R (bit/s/Hz).

5.1. Performance under presence of noise and interference

In the following, we compare the performance of the SAIC approach using the RLS algorithm and that of the conventional QAM transmission scheme for low DIR values of 0 and 5 dB, respectively. The CIR has been chosen such that both receivers yield block-error rates (BLER) below 50%. Figure 8 illustrates results for the BER after channel decoding, which indicate that for DIR = 0 dB and high $\overline{E}_b/N_0$ the proposed scheme performs better than the conventional QAM scheme except for the case of transmission with a spectral efficiency of 2.0 bit/s/Hz. This case corresponds to 8ASK transmission with code rate $R_c = 2/3$, and its performance is inferior to that of the conventional scheme with 64QAM transmission and $R_c = 1/3$ in terms of BER for DIR = 0 dB, but still acceptable. The reason for this behavior is that for ASK
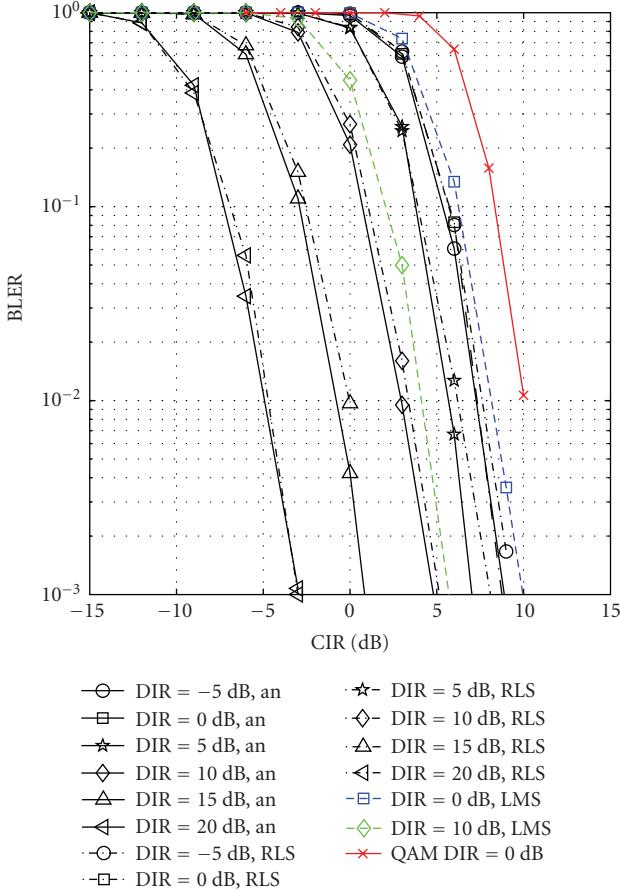
FIGURE 10: BLER after channel decoding versus CIR for varying DIR. 4ASK with $R_c = 0.5$ and 16QAM with $R_c = 0.25$, $R = 1$ bit/s/Hz. "an" stands for the analytical MMSE solution.
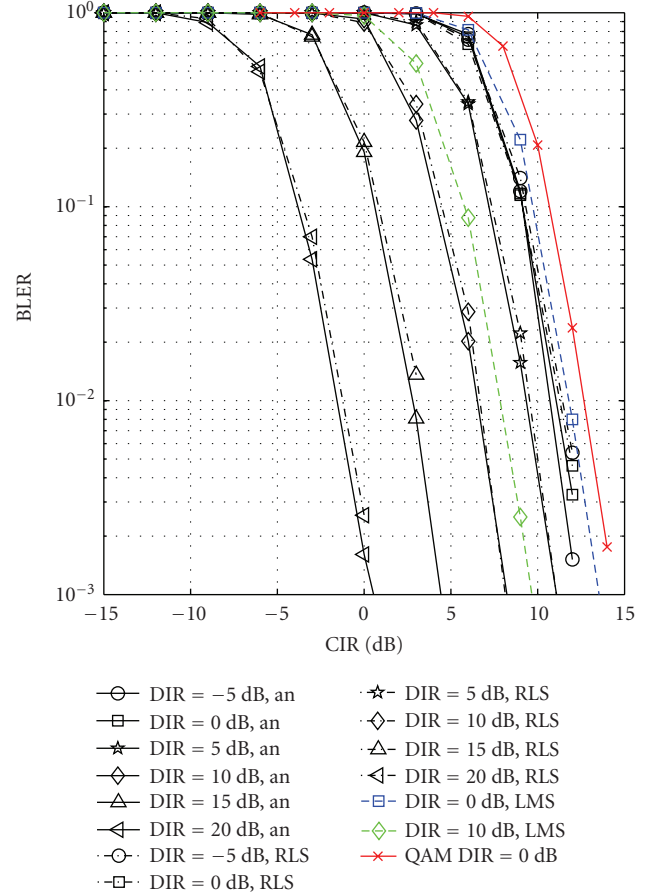

FIGURE 11: BLER after channel decoding versus CIR for varying DIR. 8ASK with $R_c = 0.5$ and 64QAM with $R_c = 0.25$, $R = 1.5$ bit/s/Hz. "an" stands for the analytical MMSE solution.

transmission the coding gain is not high enough in this case. However, also for this modulation and coding scenario an increase in DIR boosts the performance of our approach. For a DIR of at least 5 dB the conventional scheme is outperformed for high $\overline{E}_b/N_0$ by the proposed scheme at the same spectral efficiency as illustrated in Figure 8. Please note that this behavior in principle reflects the results of Section 4, where it was shown that the raw BEP of the proposed scheme is superior for moderate-to-high $\overline{E}_b/N_0$.

5.2. Performance in the interference limited case

In the following, simulation results for an interference limited scenario with $J = 3$ interferers as previously are presented. $\overline{E}_b/N_0 = 30$ dB is valid. BER and block-error rate (BLER) results are shown for the analytical MMSE solution (cf. (14)) and the adaptive solution using LMS and RLS algorithm, respectively, in Figures 9 to 12. BER results are only provided for selected cases in addition to the BLER results, which have a higher significance with respect to system performance. Results for the conventional scheme are shown only for a DIR of 0 dB. This is justified because performance

of QAM transmission is approximately independent of DIR and only depends on CIR.

From Figures 9 to 12 we observe that the proposed scheme performs better and better with increasing DIR and yields significant gains. The proposed scheme in combination with CC and interleaving outperforms the corresponding conventional QAM transmission scheme for all DIRs for 4ASK and 8ASK transmission with $R_c = 1/2$. For 8ASK with CC with $R_c = 2/3$ the proposed scheme requires a DIR ≥ 5 dB to perform superior to conventional transmission which is represented by 16QAM with $R_c = 1/2$ and 64QAM with $R_c = 1/3$ (cf. Figure 12). A DIR of 5 dB is realistic in practice assuming low shadowing correlation of different base stations. As a result of a higher diversity gain due to coding the slope of the QAM BER/BLER curves is higher than that of the corresponding curves for ASK modulation, where a higher code rate was used to obtain the same spectral efficiency. Nevertheless, ASK outperforms QAM if a certain, reasonably low DIR threshold is exceeded. For a DIR of 20 dB, that is, a highly dominant cochannel interferer is present, a gain of approximately 14 dB can be observed for 4ASK and 8ASK with $R_c = 1/2$ with respect to the conventional
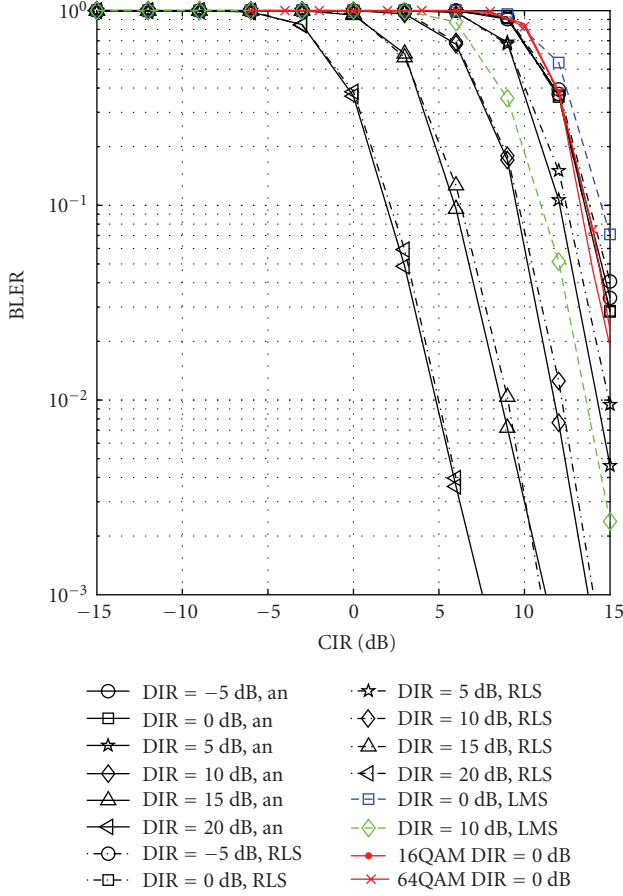
FIGURE 12: BLER versus CIR for varying DIR. 8ASK with $R_c = 0.67$, 16QAM with $R_c = 0.5$, and 64QAM with $R_c = 0.33$, $R = 2$ bit/s/Hz. "an" stands for the analytical MMSE solution.

transmission schemes and a gain of approximately 10 dB results for 8ASK with $R_c = 2/3$.

Further analysis has shown that a training length of 21 OFDM symbols is sufficient in order to obtain essentially the same performance with the adaptive RLS scheme as with the analytical MMSE solution for filter $P_i[\mu]$. This is due to the fact that the excess error induced by the RLS algorithm becomes small after a few training symbols already because of the adopted filter length of one, resulting in almost coinciding curves for both solutions. For the LMS algorithm the training length has been chosen about 10 times higher than for the RLS algorithm and still a performance loss in the order of approximately 1 dB for DIRs of 0 to 10 dB can be observed from Figures 9 to 12. Therefore, the LMS algorithm is impractical for scenarios with mobile users resulting in time-varying impulse responses. Further results not shown here demonstrate that the adaptive RLS scheme is also robust to imperfect frequency synchronization causing frequency offsets.

In summary, the performance results for the conventional QAM scheme with a DIR of 0 dB in Figures 9 to 11 are always inferior to that of the proposed scheme for spectral efficiencies of 1.0 and 1.5 bit/s/Hz. The results for a spec-

tral efficiency of 2.0 bit/s/Hz of Figure 12 show that the proposed scheme requires a DIR of at least 5 dB to outperform the conventional QAM scheme, which has been already observed from Figure 8.

6. CONCLUSIONS

A novel strategy for downlink OFDM transmission under presence of severe cochannel interference was presented, which combines coded real-valued ASK modulation and single antenna interference cancellation. Our scheme enables high downlink data rates already at low CIR values and is capable of exploiting increasing DIRs contrary to the conventional OFDM transmission scheme using QAM modulation. A comparison to QAM transmission has shown that for all modulation and coding schemes studied in this paper, the novel scheme is superior with respect to BER/BLER after channel decoding for DIRs of at least 5 dB for the same spectral efficiency R. For higher values of DIR, gains up to 14 dB have been noticed. The superior performance of the proposed scheme is confirmed by the given closed-form analysis of the raw BEP. Therefore, by exploiting the additional degrees of freedom gained by using real-valued modulation we can more than compensate for the loss in power efficiency of ASK and enable high user data rates with a blind interference suppression scheme which does not require any explicit knowledge about the interferers and is moderate in terms of computational complexity. In future work, an analytical evaluation of BER/BLER after channel coding will be made, based on the presented closed-form raw BEP results.

APPENDICES

A. MMSE SOLUTION FOR A SINGLE INTERFERER AT HIGH E_b/N_0

The MMSE solution for the projection filter $P_i[\mu]$ is given by

$$P_i[\mu] = 2\frac{\varphi_{AR}[\mu]\Phi_{RR}[\mu] - \varphi_{AR}^*[\mu]\Phi_{R^*R}[\mu]}{\Phi_{RR}^2[\mu] + |\Phi_{R^*R}[\mu]|^2}. \qquad (A.1)$$

With $J = 1$ and $\sigma_n^2 \to 0$ we can simplify $\Phi_{RR}[\mu]$ (cf. (11)) and obtain

$$\Phi_{RR}[\mu] = \mathcal{E}\{R_i[\mu]R_i^*[\mu]\} = \sigma_a^2 \cdot |H_i[\mu]|^2 + \sigma_I^2 \cdot |G_{1,i}[\mu]|^2. \qquad (A.2)$$

Expanding (A.1) by inserting the expressions for $\Phi_{RR}[\mu]$, $\varphi_{AR}[\mu]$, and $\Phi_{R^*R}[\mu]$, respectively, results in

$$P_i[\mu] = 2 \cdot \frac{\sigma_a^2 \cdot H_i^*[\mu] \cdot \left(\sigma_a^2 \cdot |H_i[\mu]|^2 + \sigma_I^2 \cdot |G_{1,i}[\mu]|^2\right)}{K[\mu] - K'[\mu]}$$
$$- \frac{\sigma_a^2 \cdot H_i[\mu] \cdot \left(\sigma_a^2 \cdot (H_i^*[\mu])^2 + \sigma_I^2 \cdot (G_{1,i}^*[\mu])^2\right)}{K[\mu] - K'[\mu]},$$

$$(A.3)$$

where

$$K[\mu] = \left(\sigma_a^2 \cdot \left|H_i[\mu]\right|^2 + \sigma_I^2 \cdot \left|G_{1,i}[\mu]\right|^2\right)^2,$$

$$K'[\mu] = \left|\sigma_a^2 \cdot (H_i^*[\mu])^2 + \sigma_I^2 \cdot (G_{1,i}^*[\mu])^2\right|^2. \tag{A.4}$$

We can simplify this expression and obtain

$$
\begin{aligned}
P_i[\mu] &= -2\frac{\sigma_a^2 \cdot \sigma_I^2 \cdot G_{1,i}^*[\mu]}{\sigma_a^2 \cdot \sigma_I^2} \cdot \frac{\left(H_i^*[\mu]G_{1,i}[\mu] - H_i[\mu]G_{1,i}^*[\mu]\right)}{\left(H_i^*[\mu]G_{1,i}[\mu] - H_i[\mu]G_{1,i}^*[\mu]\right)^2} \\
&= -\frac{G_{1,i}^*[\mu]}{(1/2)\left(H_i^*[\mu]G_{1,i}[\mu] - H_i[\mu]G_{1,i}^*[\mu]\right)} \\
&= -j \cdot \frac{G_{1,i}^*[\mu]}{\mathrm{Im}\{H_i[\mu]G_{1,i}^*[\mu]\}}.
\end{aligned}
\tag{A.5}
$$

B. THE SOLUTION TO THE DOUBLE INTEGRAL

We aim at solving the following double integral:

$$\frac{1}{\sqrt{\pi x}}\frac{2}{\pi}\int_0^{\pi/2}\int_0^\infty \frac{\exp\left(-(\alpha G(M)y/\sin^2(\theta))\right)\cdot \exp\left(-(y/x)\right)}{\sqrt{y}}\,dy\,d\theta, \tag{B.1}$$

where $\alpha \in \mathbb{R}^+$. The inner integral has the solution [26]

$$
\begin{aligned}
&\int_0^\infty \frac{\exp\left(-(\alpha G(M)y/\sin^2(\theta))\right)\cdot \exp\left(-(y/x)\right)}{\sqrt{y}}\,dy \\
&= \frac{\Gamma(1/2)}{\sqrt{1/x + (\alpha G(M)/\sin^2(\theta))}} \\
&= \sqrt{\pi}\frac{\sqrt{x}\sin\theta}{\sqrt{\alpha G(M)x + \sin^2\theta}} \quad \text{for } 0 \le \theta \le \frac{\pi}{2},
\end{aligned}
\tag{B.2}
$$

where $\Gamma(1/2) = \sqrt{\pi}$ has been used [28]. Subsequent outer integration yields

$$
\begin{aligned}
&\int_0^{\pi/2} \frac{\sqrt{x}\sin\theta}{\sqrt{\alpha G(M)x + \sin^2\theta}}\,d\theta \\
&= \frac{1}{2}\sqrt{x}\arctan\left(\frac{1}{2}\frac{\alpha G(M)x + 1 - 2\cos^2\theta}{\cos\theta\sqrt{1 + \alpha G(M)x - \cos^2\theta}}\right)\Bigg|_0^{\pi/2} \\
&= \frac{1}{2}\sqrt{x}\left(\frac{\pi}{2} - \arctan\left(\frac{\alpha G(M)x - 1}{2\sqrt{\alpha G(M)x}}\right)\right),
\end{aligned}
\tag{B.3}
$$

which can be proved by means of differentiation of the second expression. Hence, the solution to the complete double integral is given by

$$\frac{1}{2}\left(1 - \frac{2}{\pi}\arctan\left(\frac{\alpha G(M)x - 1}{2\sqrt{\alpha G(M)x}}\right)\right). \tag{B.4}$$

C. BEP OF QAM TRANSMISSION OVER A RAYLEIGH FADING CHANNEL

The exact bit-error probabilities for transmission over the AWGN channel with 4QAM, 16QAM, and 64QAM modulation, respectively, can be expressed as [24]

$$
\begin{aligned}
P_b^{4\mathrm{QAM}}(\widetilde{y}) &= \frac{1}{2}\cdot\mathrm{erfc}\left(\sqrt{\widetilde{G}(4)\widetilde{y}}\right), \\
P_b^{16\mathrm{QAM}}(\widetilde{y}) &= \frac{3}{8}\cdot\mathrm{erfc}\left(\sqrt{\widetilde{G}(16)\widetilde{y}}\right) \\
&\quad + \frac{1}{4}\cdot\mathrm{erfc}\left(\sqrt{9\widetilde{G}(16)\widetilde{y}}\right) \\
&\quad - \frac{1}{8}\cdot\mathrm{erfc}\left(\sqrt{25\widetilde{G}(16)\widetilde{y}}\right), \\
P_b^{64\mathrm{QAM}}(\widetilde{y}) &= \frac{7}{24}\cdot\mathrm{erfc}\left(\sqrt{\widetilde{G}(64)\widetilde{y}}\right) \\
&\quad + \frac{1}{4}\cdot\mathrm{erfc}\left(\sqrt{9\widetilde{G}(64)\widetilde{y}}\right) \\
&\quad - \frac{1}{24}\cdot\mathrm{erfc}\left(\sqrt{25\widetilde{G}(64)\widetilde{y}}\right) \\
&\quad + \frac{1}{24}\cdot\mathrm{erfc}\left(\sqrt{81\widetilde{G}(64)\widetilde{y}}\right) \\
&\quad - \frac{1}{24}\cdot\mathrm{erfc}\left(\sqrt{169\widetilde{G}(64)\widetilde{y}}\right),
\end{aligned}
\tag{C.1}
$$

where $\widetilde{y}$ is the instantaneous subcarrier E_b/N_0 and $\widetilde{G}(M) = (6\log_2 M/4(M-1))$ ($\widetilde{G}(4) = 1$, $\widetilde{G}(16) = 2/5$, $\widetilde{G}(64) = 1/7$). The expected BEP for transmission over a Rayleigh fading channel versus $x = \overline{E}_b/N_0$ is therefore

$$\overline{P}_b(x) = \int_0^\infty P_b(\widetilde{y})f_{\widetilde{y}}(\widetilde{y})\,d\widetilde{y}. \tag{C.2}$$

Please note that the M^2-ary QAM superscripts have been omitted for simplicity, here. This integral can be solved in closed form for all M^2-ary QAM constellations. Using $\widetilde{y} = \xi \cdot x$ and $f_\xi(\xi) = e^{-\xi}$ the pdf of $\widetilde{y}$ is expressed as

$$f_{\widetilde{y}}(\widetilde{y}) = \frac{e^{-\widetilde{y}/x}}{x}. \tag{C.3}$$

Then, in order to determine the BEPs for M^2-ary QAM transmission over a Rayleigh fading channel the following identity is needed:

$$
\begin{aligned}
&\int_0^\infty \mathrm{erfc}\left(\alpha\widetilde{G}(M)x\right)\frac{e^{-\widetilde{y}/x}}{x}\,d\widetilde{y} \\
&= \frac{2}{\pi x}\int_0^{\pi/2}\int_0^\infty \exp\left(-\widetilde{y}\left(\frac{\alpha\widetilde{G}(M)x + \sin^2\theta}{x\sin^2\theta}\right)\right)\,d\widetilde{y}\,d\theta \\
&= \frac{2}{\pi}\int_0^{\pi/2}\frac{\sin^2\theta}{\alpha\widetilde{G}(M)x + \sin^2\theta}\,d\theta = 1 - \sqrt{\frac{\alpha\widetilde{G}(M)x}{1 + \alpha\widetilde{G}(M)x}},
\end{aligned}
\tag{C.4}
$$

where the solution to the inner integral can be found in [26] and the solution for the outer integral is implicitly stated in

[19]. Therefore, the average BEP for 4QAM, 16QAM, and 64QAM, respectively, is

$$P_b^{4\text{QAM}}(x) = \frac{1}{2}\left(1 - \sqrt{\frac{x}{1+x}}\right),$$

$$P_b^{16\text{QAM}}(x) = \frac{3}{8}\left(1 - \sqrt{\frac{(2/5)x}{1+(2/5)x}}\right)$$
$$+ \frac{1}{4}\left(1 - \sqrt{\frac{(18/5)x}{1+(18/5)x}}\right)$$
$$- \frac{1}{8}\left(1 - \sqrt{\frac{10x}{1+10x}}\right),$$

$$P_b^{64\text{QAM}}(x) = \frac{7}{24}\left(1 - \sqrt{\frac{(1/7)x}{1+(1/7)x}}\right) \qquad \text{(C.5)}$$
$$+ \frac{1}{4}\left(1 - \sqrt{\frac{(9/7)x}{1+(9/7)x}}\right)$$
$$- \frac{1}{24}\left(1 - \sqrt{\frac{(25/7)x}{1+(25/7)x}}\right)$$
$$+ \frac{1}{24}\left(1 - \sqrt{\frac{(81/7)x}{1+(81/7)x}}\right)$$
$$- \frac{1}{24}\left(1 - \sqrt{\frac{(169/7)x}{1+(169/7)x}}\right).$$

REFERENCES

[1] 3GPP, "Physical layer aspects for evolved utra (V7.1.0)," Tech. Rep. TR 25.814, 3rd Generation Partnership Project (3GPP), 2006.

[2] IEEE Std 802.16e, "IEEE standard for local and metropolitan area networks, part 16: air Interface for fixed and mobile broadband wireless access systems," Tech. Rep., IEEE, 2006.

[3] Y. Li and N. R. Sollenberger, "Adaptive antenna arrays for OFDM systems with cochannel interference," *IEEE Transactions on Communications*, vol. 47, no. 2, pp. 217–229, 1999.

[4] B.-S. Seo, S.-G. Choi, and J.-S. Cha, "Maximum ratio combining for OFDM systems with cochannel interference," *IEEE Transactions on Consumer Electronics*, vol. 52, no. 1, pp. 87–91, 2006.

[5] S. Kapoor, D. J. Marchok, and Y.-F. Huang, "Adaptive interference suppression in multiuser wireless OFDM systems using antenna arrays," *IEEE Transactions on Signal Processing*, vol. 47, no. 12, pp. 3381–3391, 1999.

[6] L. Giangaspero, L. Agarossi, G. Paltenghi, S. Okamura, M. Okada, and S. Komaki, "Co-channel interference cancellation based on MIMO OFDM systems," *IEEE Wireless Communications*, vol. 9, no. 6, pp. 8–17, 2002.

[7] J. Li, K. B. Letaief, and Z. Cao, "Co-channel interference cancellation for space-time coded OFDM systems," *IEEE Transactions on Wireless Communications*, vol. 2, no. 1, pp. 41–49, 2003.

[8] P. Tan and N. C. Beaulieu, "An improved MMSE equalizer for one-dimensional modulation OFDM systems," in *Proceedings of the Vehicular Technology Conference (VTC '05)*, pp. 157–160, September 2005.

[9] P. Chevalier and F. Pipon, "New insights into optimal widely linear array receivers for the demodulation of BPSK, MSK, and GMSK signals corrupted by noncircular interferences—application to SAIC," *IEEE Transactions on Signal Processing*, vol. 54, no. 3, pp. 870–883, 2006.

[10] H. Trigui and D. T. M. Slock, "Cochannel interference cancellation within the current GSM standard," in *Proceedings of the International Conference on Personal Communications (ICUPC '98)*, 1998.

[11] M. Pukkila, G. P. Mattellini, and P. A. Ranta, "Cochannel interference suppression for constant modulus signals," in *Proceedings of the IEEE International Conference on Communications*, vol. 5, pp. 2548–2552, 2004.

[12] A. Mostafa, R. Kobylinski, I. Kostanic, and M. Austin, "Single Antenna Interference Cancellation (SAIC) for GSM networks," in *Proceedings of the IEEE Vehicular Technology Conference (VTC '04)*, vol. 2, pp. 1089–1093, October 2004.

[13] R. Meyer, W. H. Gerstacker, R. Schober, and J. B. Huber, "A single antenna interference cancellation algorithm for GSM," in *Proceedings of the IEEE Vehicular Technology Conference (VTC '05)*, vol. 2, pp. 821–825, Stockholm, Sweden, May-June 2005.

[14] R. Meyer, W. Gerstacker, and R. Schober, "Method for Cancelling Interference during TDMA Transmission and/or FDMA Transmission," International Patent Application WO02/054660A1, PCT/EP01/15019 (granted), 2000.

[15] R. Meyer, W. H. Gerstacker, R. Schober, and J. B. Huber, "A single antenna interference cancellation algorithm for increased GSM capacity," *IEEE Transactions on Wireless Communications*, vol. 5, no. 7, pp. 1616–1621, 2006.

[16] A. Lampe and M. Breiling, "Asymptotic analysis of widely linear MMSE multiuser detection—complex vs. real modulation," in *Proceedings of IEEE Information Theory Workshop (ITW '01)*, September 2001.

[17] D. Darsena, G. Gelli, L. Paura, and F. Verde, "Widely linear equalization and blind channel identification for interference-contaminated multicarrier systems," *IEEE Transactions on Signal Processing*, vol. 53, no. 3, pp. 1163–1177, 2005.

[18] S. Verdú, *Multiuser Detection*, Cambridge University Press, New York, NY, USA, 1998.

[19] K. D. Kammeyer, *Nachrichtenübertragung*, Teubner, Stuttgart, Germany, 3rd edition, 2004.

[20] R. Rebhan and J. Zander, "On the outage probability in single frequency networks for digital broadcasting," *IEEE Transactions on Broadcasting*, vol. 39, no. 4, pp. 395–401, 1993.

[21] N. Benvenuto and G. Cherubini, *Algorithms for Communications Systems and Their Applications*, Wiley, New York, NY, USA, 2002.

[22] J. Bendat and A. G. Persol, *Random Data, Analysis and Measurement Procedures*, Wiley, New York, NY, USA, 1986.

[23] J. G. Proakis, *Digital Communications*, McGraw-Hill, Boston, Mass, USA, 2001.

[24] K. Cho and D. Yoon, "On the general BER expression of one- and two-dimensional amplitude modulations," *IEEE Transactions on Communications*, vol. 50, no. 7, pp. 1074–1080, 2002.

[25] C. Tellambura and A. Annamalai, "Derivation of Craig's formula for Gaussian probability function," *Electronics Letters*, vol. 35, no. 17, pp. 1424–1425, 1999.

[26] G. Grosche, V. Ziegler, and D. Ziegler, *Taschenbuch der Mathematik*, Verlag Harri Deutsch, Frankfurt, Germany, 1985.

[27] M. Failli, *COST 207 Digital Land Mobile Radio Communications*, Commission of the European Communities, 1989.

[28] T. K. Moon and W. C. Stirling, *Mathematical Methods and Algorithms for Signal Processing*, Prentice-Hall, Upper Saddle River, NJ, USA, 2000.